Journal of Zhejiang University SCIENCE A
ISSN 1673-565X (Print); ISSN 1862-1775 (Online)
www.zju.edu.cn/jzus; www.springerlink.com
E-mail: jzus@zju.edu.cn

A New Technique:

Research and industrial application of a novel compound permanent magnet synchronous machine*

Cheng-zhi FAN†, Ming-xing HUANG†‡, Yun-yue YE

(*School of Electrical Engineering, Zhejiang University, Hangzhou 310027, China*)

†E-mail: fanchengzhi@zju.edu.cn; minshing@zju.edu.cn

Received Nov. 12, 2008; Revision accepted Feb. 3, 2009; Crosschecked Feb. 16, 2009

Abstract: We propose a novel kind of compound permanent magnet synchronous machine (CPMSM), which is applicable in low-speed and high-torque situations. We first explain the structure of the CPMSM. Based on theoretically deducing the calculation formulae of the CPMSM electromagnetic parameters, we analyze the operating characteristics of the CPMSM, and obtain the power-angle curves and working curves. The no-load magnetic field distribution and the cogging torque are analyzed by applying the finite element method of three-dimensional (3D) magnetic fields, to determine the no-load leakage coefficient and the waveform of the cogging torque. Furthermore, the optimal parameters of the permanent magnet for reducing the cogging torque are determined. An important application target of the CPMSM is in direct-drive pumping units. We have installed and tested a direct-drive pumping unit in an existing oil well. Test results show that the power consumption of the direct-drive pumping unit driven by CPMSM is 61.1% of that of the beam-pumping unit, and that the floor space and weight are only 50% of those of a beam-pumping unit. The noise output does not exceed 58 dB in a range of 1 m around the machine when the machine is 1.5 m from the ground.

Key words: Compound permanent magnet synchronous machine (CPMSM), Operating characteristic, Three-dimensional finite element analysis, Cogging torque, Direct-drive pumping unit

doi:10.1631/jzus.A0820789 **Document code:** A **CLC number:** TM351

STRUCTURE AND FORMULAE DEDUCTION OF CPMSM

In many industrial applications, the high-speed motion of electric machines needs to be transformed into low-speed motion with increased output torque. A common means of speed reduction is a reducing mechanism such as a reduction gearbox. Due to the low efficiency of this kind of reducing mechanism, the efficiency of the drive system decreases and the power consumption of the electric machine increases. A low-speed electric machine that can output large torque is better suited to these situations because it can improve the efficiency of the drive system and decrease power consumption.

Direct-drive low-speed electric machines that combine the structure of external-rotor electric machines and disk electric machines (compound permanent magnet synchronous machines, CPMSM) can increase the output torque. The stator of a CPMSM consists of one cylindrical stator and two disk stators; the rotor of a CPMSM is a totally enclosed structure that combines a cylindrical rotor with a disk rotor. The stator is attached to the main shaft, which is fixed to the base; the rotor can rotate around the shaft by means of bearings. Two drums on which the steel cables can be wrapped are fixed to the bilateral disk type rotors (Fig.1) (Gieras and Wing, 1997; Tang, 1997; Huang *et al*., 2007).

The stator windings of the CPMSM are numerous, and the windings of the cylindrical stator are perpendicular to the windings of the disk stator. To enable three sub-machines to operate synchronously using the same electrical supply, the windings of the three sub-machines should be connected to the electrical supply in series.

‡ Corresponding author

* Project (No. 50607016) supported by the National Natural Science Foundation of China

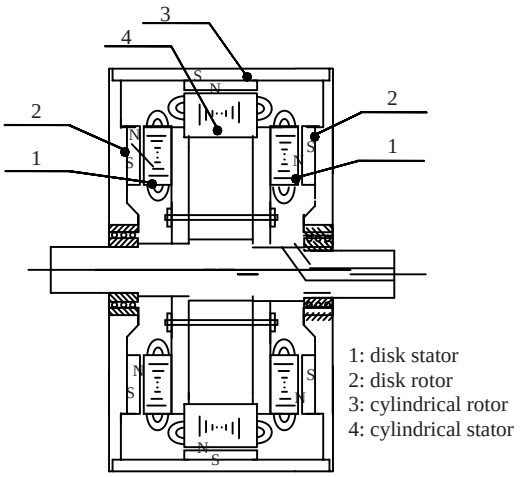

Fig.1 Structure of the compound permanent magnet synchronous machine (CPMSM)

The rotor of the CPMSM has the structure of surface mounted permanent magnets. Its direct-axis reactance is almost equal to the quadrature-axis reactance, i.e., $X_d \approx X_q$. So the synchronous reactance X_t can replace the direct-axis reactance X_d and the quadrature-axis reactance X_q, and can be expressed as

$$X_t = X_m + X_\sigma, \tag{1}$$

where X_m is the principal reactance and X_σ is the leakage reactance.

From the phasor diagram of a permanent magnet synchronous machine (PMSM), the following formulae can be summarized:

$$\psi = \arctan(I_d / I_q), \tag{2a}$$

$$U\sin\theta = r_1 I_d + X_t I_q, \tag{2b}$$

$$U\cos\theta = E_0 + r_1 I_q - X_t I_d, \tag{2c}$$

where U is the external phase voltage, E_0 is the no-load back electromotive force, I_d and I_q are the direct- and quadrature-axis components of stator phase current respectively, r_1 is the stator direct current resistance, θ is the power-angle of the PMSM, and ψ is the inner power factor angle. From Eqs.(2a) and (2b), the expressions of I_d and I_q can be deduced as follows:

$$I_d = \frac{r_1 U\sin\theta + X_t(E_0 - U\cos\theta)}{r_1^2 + X_t^2}, \tag{3a}$$

$$I_q = \frac{X_t U\sin\theta - r_1(E_0 - U\cos\theta)}{r_1^2 + X_t^2}. \tag{3b}$$

The expression of stator phase current is

$$I = \sqrt{I_d^2 + I_q^2}. \tag{4}$$

By substituting Eqs.(3a) and (3b) into Eq.(4), we have

$$I^2 = \frac{U^2 + E_0^2 - 2UE_0\cos\theta}{r_1^2 + X_t^2}. \tag{5}$$

Eq.(5) is a simple quadratic equation about U. The roots of Eq.(5) are $E_0\cos\theta \pm [I^2(r_1^2 + X_t^2) - E_0^2\sin^2\theta]^{1/2}$. Because E_0 is usually less than U for obtaining a higher power factor, and $\cos\theta<1$, the rational root of U should be

$$U = E_0\cos\theta + \sqrt{I^2(r_1^2 + X_t^2) - E_0^2\sin^2\theta}. \tag{6}$$

The external voltage of the cylindrical stator is U_1, which is a little higher than the no-load back electromotive force E_{01} of the cylindrical stator. The power angle of the cylindrical part should be equal to the power angle of the disk part. After setting the power angle, the stator current of the cylindrical part can be worked out according to Eqs.(3) and (4), which is also equal to the stator current of the disk part. As the power angle and the stator current of the disk part are known, the external voltage U_2 of a single disk stator can be worked out according to Eq.(6). So the total external voltage of the CPMSM is

$$U = U_1 + 2U_2. \tag{7}$$

According to the definition of PMSM, the input power P_1 can be expressed as

$$P_1 = mUI\cos\varphi = m(UI_d\sin\theta + UI_q\cos\theta), \tag{8}$$

where φ is the power factor angle. Furthermore, there is the equation $\varphi=\psi-\theta$. Substitution of Eqs.(2b), (2c) and (4) into Eq.(8) results in

$$P_1 = m(I^2 r_1 + E_0 I_q). \tag{9}$$

Because the electromagnetic power P_{em} is the difference between the input power P_1 and the stator winding loss $p_{Cu}=mI^2r_1$, the expression of P_{em} can be derived as follows while considering Eq.(3b):

$$P_{\mathrm{em}}=\frac{mE_0}{r_1^2+X_{\mathrm{t}}^2}(X_{\mathrm{t}}U\sin\theta+r_1U\cos\theta-r_1E_0). \quad (10)$$

The outline dimension of the CPMSM is much larger than that of a common PMSM. Because the rated frequency of the CPMSM is usually less than 15 Hz, the synchronous reactance X_{t} is correspondingly small, and the ratio with the stator direct current resistance r_1 is not large. So the r_1 in Eq.(10) cannot be ignored (Dou and Liu, 2004; Chen *et al*., 2005; Rieder and Schroedl, 2005; Aydin *et al*., 2006).

OPERATING CHARACTERISTICS OF CPMSM

When the no-load leakage coefficients of the cylindrical part and the disk part are calculated, the magnetic circuit of the whole electric machine can be decompounded into two independent parts, the cylindrical part and the disk part. The electric circuit parameters can also be decompounded to calculate values such as r_1 and E_0. The parameters of a model of the CPMSM for the cylindrical part and the disk part are shown in Table 1.

Table 1 Parameters of the model machine

Parameter	Cylindrical part	Disk part
Air gap, δ (mm)	3	3
Length of the motor, L_{ef} (mm)	350	100
Thickness of the PM, h_{M} (mm)	10	10
EMF, E_0 (V)	183.7	9.2*
Synchronous reactance, X_{t} (Ω)	3.875	0.196*
Main reactance, X_{m} (Ω)	3.196	0.140*
Stator direct current resistance, r_1 (Ω)	1.53#	0.29*#

Parameter	Whole electric machine
Rated voltage, U_{Nl} (V)	380
Rated current, I_{N} (A)	22.9
Rated torque, T_{N} (N·m)	8786
Rated power, P_{N} (kW)	11.5
Rated frequency, f (Hz)	5
Number of poles, p	24
External diameter of the CPMSM, D_2 (mm)	1200

* Single disk; # Hot condition; *# Single disk & hot condition

The power-angle curve of the model machine can be worked out according to Eq.(10) (Fig.2). It can be seen that the power angle for obtaining the maximal electromagnetic power $P_{\mathrm{em\,max}}$ is about 66°, which is different from the power angle of common non-salient synchronous machines (almost 90°). The reason can be found from the following formula:

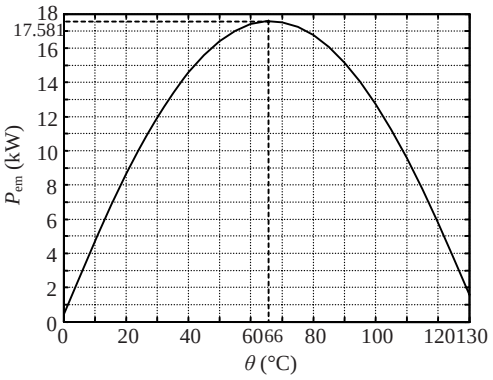

Fig.2 Power-angle curve of the model machine

$$\frac{\mathrm{d}P_{\mathrm{em}}}{\mathrm{d}\theta}=\frac{mE_0}{r_1^2+X_{\mathrm{t}}^2}(X_{\mathrm{t}}U\cos\theta-r_1U\sin\theta). \quad (11)$$

By setting $\frac{\mathrm{d}P_{\mathrm{em}}}{\mathrm{d}\theta}=0$, the following result can be obtained from Eq.(11):

$$\tan\theta=X_{\mathrm{t}}/r_1. \quad (12)$$

The rated frequency of the model machine is 5 Hz. From Table 1, the values of other parameters can be obtained, i.e., X_{t}=3.875+2×0.196=4.267 Ω, r_1=1.53+2×0.29=2.11 Ω. Then, according to Eq.(12), θ=63.7°. On the whole, the results accord with the power-angle curve.

Fig.3 shows the curves of per unit input power P_1/P_{N}, per unit output power P_2/P_{N}, per unit output torque T/T_{N}, per unit stator current I/I_{N}, power factor $\cos\varphi$, and efficiency η with variable power angle θ. The curves of P_2/P_{N} and T/T_{N} are almost overlapping and have maximal values, which are equal to multiples of the pull-out torque, when the power angle is 65°. The calculated maximal output power $P_{2\mathrm{max}}$ and maximal output torque T_{max} are 16.76 kW and 12.8 kN·m, respectively. The curve of P_1/P_{N} has an almost monotonic rise and a maximal value of $P_{1\mathrm{max}}$=44.13 kW, when the power angle is 120°. The curve of I/I_{N} has an approximately linear rise from 0° to 130°, which causes the stator winding loss to increase like a quadratic curve. The curve of η decreases gradually, and falls to 0 when the power angle is 130°.

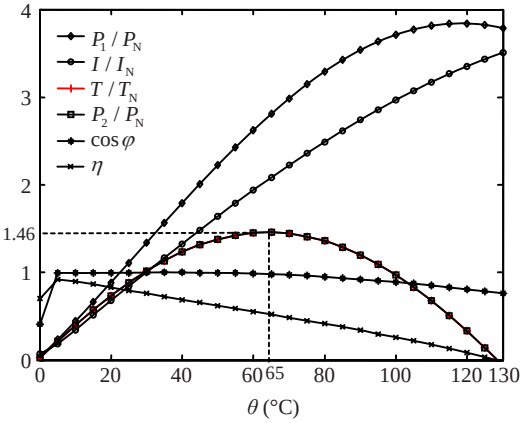

Fig.3 Working curves of the model machine

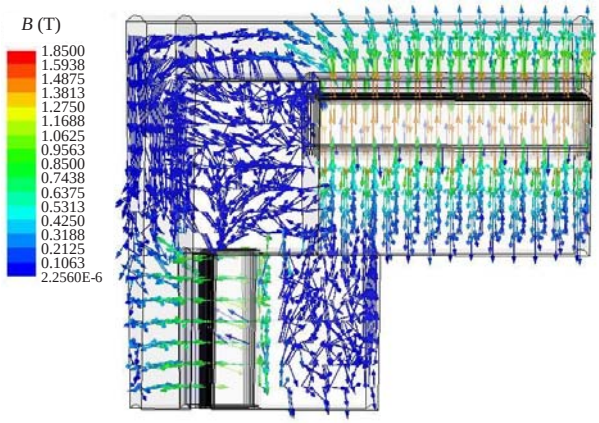

Fig.4 Plot of magnetic flux density vector

ANALYSIS OF 3D MAGNETIC FIELD AND COGGING TORQUE

Finite element analysis of 3D magnetic fields

Because there is magnetic flux leakage between the cylindrical part and the two disk parts of the CPMSM, finite element analysis of the 3D magnetic field for the CPMSM is necessary. A finite element model of the CPMSM was built, consisting of stators and rotors of half of a cylindrical part and a disk part in a pair of poles range. Fig.4 shows the plot of the magnetic flux density vector in the CPMSM when the electric machine is no-load running. The magnetic flux density of the junction between the cylindrical part and the disk part in the rotor yoke is almost less than 0.1 T. According to the results of finite element analysis, the total magnetic flux offered by each permanent magnet pole is 0.023 03 Wb, and the main magnetic flux in the air-gap is 0.018 55 Wb in the cylindrical part. So the no-load leakage coefficient of the cylindrical part is about 1.24. Likewise, the total magnetic flux offered by each permanent magnet pole is 0.004 498 Wb, and the main magnetic flux in the air-gap is 0.003 176 Wb in the single disk part. So the no-load leakage coefficient of the single disk part is about 1.41 (Howe and Zhu, 1992; Aydin *et al*., 2001; Qu and Lipo, 2002).

Analysis of cogging torque

As a result of the influence of cogging torque on the PMSM, the CPMSM suffers greater torque fluctuation during low-speed operation, which is disadvantageous for the stability of the driving load. So, one of the main concerns in the design of CPMSM is how to reduce cogging torque effectively. The effect of the pole-arc coefficient or the angle of skewed permanent magnet on reducing cogging torque is discussed below. The analysis of the CPMSM is divided into two parts: the cylindrical electric machine and the disk electric machine (Bianchi and Bolognani, 2002; Gieras, 2004; Lateb *et al.*, 2006; Yang *et al.*, 2006).

With the 3D finite element method of transient field analysis, the cogging torque waveform of the cylindrical electric machine is determined in a pitch of stator teeth range when α_p is 0.667 and 0.733 (Fig.5a). At the same time, the cogging torque waveform of the disk electric machine is also determined in a pitch of stator teeth range when α_p is 0.533, 0.600, 0.667, 0.733, 0.800, and 0.867 (Fig.5b). The smallest cogging torque is obtained when, α_p is 0.667 for the cylindrical electric machine, and α_p is 0.533 or 0.800 for the disk electric machine.

The method of skewed PM is a simple and effective way to reduce the cogging torque. For the cylindrical and disk parts of the CPMSM, the cogging torque waveform was determined in a pitch of stator teeth range when the angle of skewed PM is the central angle corresponding to 0, 0.4, 0.6, 0.8, 1.0, and 1.2 pitch(es) of teeth (Figs.6a and 6b). For both electric machines, when the angle of skewed PM is the central angle corresponding to 1.0 pitch of teeth, the cogging torque is minimized and is much smaller than that of non-skewed PM.

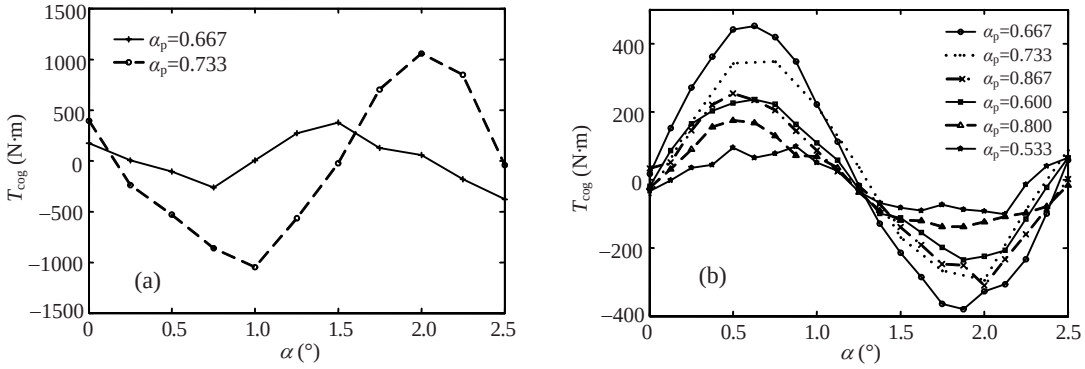

Fig.5 Comparison of cogging torque (T_{cog}) and α_p in a cylindrical electric machine (a) and a disk electric machine (b)

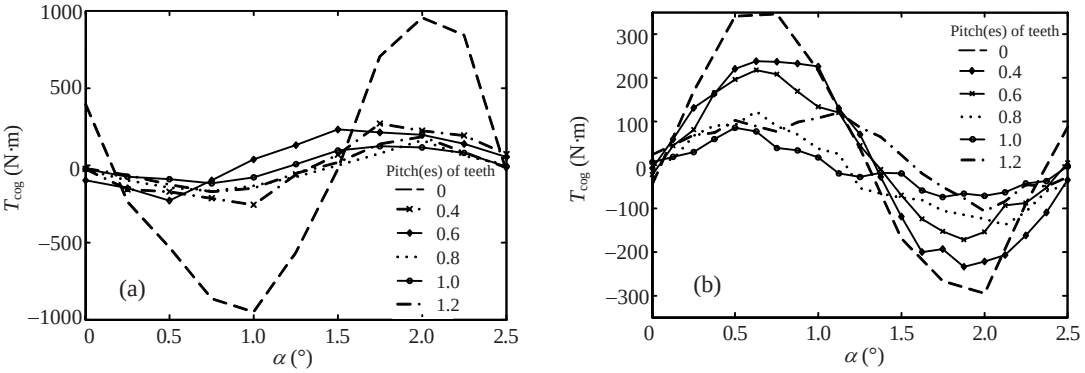

Fig.6 Comparison of cogging torque (T_{cog}) and angle of skewed PM in a cylindrical electric machine (a) and a disk electric machine (b)

APPLICATION IN DIRECT-DRIVE PUMP UNITS

Direct-drive pumping units in which the core is the CPMSM are used in oil extraction equipment. Compared with traditional beam pumping units, direct-drive pumping units cut out many transmission mechanisms such as belt pulleys, reduction gearboxes, cranks, connecting rods, and beams. Instead, they need only a reel-pumping rod and a balance weight on both sides of the electric machine attached using steel cables or high strength belts (Fig.7). In a direct-drive pumping unit, when the CPMSM rotates, the pumping rod and balance weights move up and down as well.

A direct-drive pumping unit has already been installed and tested in an existing oil well. The parameters of the CPMSM are shown in Table 1. Table 2 shows a comparison by authoritative measurement departments of current, efficiency and power consumption between the direct-drive pumping unit and the beam-pumping unit in the same oil well (Li *et al.*, 2001; Yu *et al.*, 2005; Bai and Zhang, 2007).

The rated power of the CPMSM in direct-drive pumping units is much lower than that of induction electric machines in beam pumping units (Table 2). This advantage changes the phenomenon of "a big horse pulls a small carriage" in pumping units. Compared with the beam-pumping unit, the direct-drive pumping unit has lower drive current and higher system efficiency. Furthermore, the direct-drive pumping unit also has the advantages of higher oil output, lighter weight, less floor area and lower noise. According to measurement, the floor space and weight of the direct-drive pumping unit are only 50% of those of the beam-pumping unit. The noise output is also much lower than that of the beam-pumping unit and does not exceed 58 dB in a range of 1 m around the machine when the machine is 1.5 m from the ground.

Fig.7 Photograph of the direct-drive pumping unit installed in an existing oil well

Table 2 Comparison of efficiency and power consumption for two kinds of pumping unit

Parameter	Direct-drive pumping unit	Beam pumping unit
Rated power (kW)	11.5	45
Average voltage (V)	238.8	238.6
Average current (A)	7.15	37.40
System efficiency (%)	61.3	40.3
Volume of production (m^3/d)	16.7	15.2
Active power consumption per 1 t & 100 m pumping [kW·h/(100 m·t)]	0.544	1.180
Reactive power consumption per 1 t & 100 m pumping [kV·A·h/(100 m·t)]	0.508	6.774
Active power energy-saving ratio $[(p_b-p_d)/p_b]$ (%)*	53.9	
Reactive power energy-saving ratio $[(q_b-q_d)/q_b]$ (%)#	92.5	
Synthesis energy-saving ratio $\left[\frac{p_b-p_d+0.04(q_b-q_d)}{p_b+0.04q_b}\right]$ (%)*#	61.1	

* p_d=0.544, p_b=1.180; # q_d=0.508, q_b=6.774

CONCLUSION

A CPMSM increases output torque per unit volume because it combines one cylindrical outer-rotor electric machine with two disk electric machines in 3D space. Because of its special structure, the operating characteristics of the CPMSM differ from those of a common PMSM. So the design formulae of the CPMSM need to be specially deduced. From the above analysis it can be seen that the output power of the CPMSM is not large, but the output torque is large. The CPMSM has the characteristics of low-speed and high-torque, and is very well suited for applications such as pumping oil in oil fields.

Direct-drive pumping units driven by the CPMSM not only greatly simplify the structure of beam pumping units, but also have a very prominent effect on power saving. The advantages of simplifying the structure are reducing the weights of the pumping units and the repair and maintenance costs. Direct-drive pumping units save energy not only by greatly decreasing active power, but also by overcoming the shortcomings of beam pumping units, such as a low power factor and large reactive power.

References

Aydin, M., Huang, S., Lipo, T.A., 2001. Optimum Design and 3-D Finite Element Analysis of Non-slotted and Slotted Internal Rotor Type Axial Flux PM Disc Machines. Proc. IEEE-PES Summer Meeting, Canada, p.1409-1416.

Aydin, M., Huang, S., Lipo, T.A., 2006. Torque quality and comparison of internal and external rotor axial flux surface-magnet disc machines. *IEEE Trans. Ind. Electron.*, **53**(3):822-830. [doi:10.1109/TIE.2006.874268]

Bai, L.P., Zhang, S.Z., 2007. Field testing method study of operational efficiency for pumping unit motors. *China Petrol. Mach.*, **35**(4):64-66 (in Chinese).

Bianchi, N., Bolognani, S., 2002. Design techniques for reducing the cogging torque in surface-mounted PM motors. *IEEE Trans. Ind. Appl.*, **38**(5):1259-1265. [doi:10.1109/TIA.2002.802989]

Chen, Y.S., Zhu, Z.Q., Howe, D., 2005. Calculation of *d*- and *q*-axis inductances of PM brushless ac machines accounting for skew. *IEEE Trans. Magn.*, **41**(10):3940-3942. [doi:10.1109/TMAG.2005.854976]

Dou, M.F., Liu, W.G., 2004. On design high-efficiency and energy-saving REPMSM (rare earth permanent magnet synchronous motor) for use in Chinese oil fields. *J. Northwestern Polytech. Univ.*, **22**(3):355-359 (in Chinese).

Gieras, J.F., 2004. Analytical approach to cogging torque calculation of PM brushless motors. *IEEE Trans. Ind. Appl.*, **40**(5):1310-1316. [doi:10.1109/TIA.2004.834108]

Gieras, J.F., Wing, M., 1997. Permanent Magnet Motor Technology. Marcel Dekker, Inc., New York, USA, p.85-105.

Howe, D., Zhu, Z.Q., 1992. Magnetic Field Analysis of Permanent Magnet Machines. Proc. 12th Int. Workshop on Rare-earth Magnets and Their Applications, p.308-337.

Huang, M.X., Fan, C.Z., Ye, Y.Y., 2007. Design and analysis of the novel compound permanent magnet synchronous motor. *Electr. Mach. Control Appl.*, **34**(10):1-4, 26 (in Chinese).

Lateb, R., Takorabet, N., Meibody, F.T., 2006. Effect of magnet segmentation on the cogging torque in surface-mounted permanent-magnet motors. *IEEE Trans. Magn.*, **42**(3):442-445. [doi:10.1109/TMAG.2005.862756]

Li, L.Y., Cui, S.M., Zheng, P., Guo, X.C., Cheng, S.K., Wang, Y., 2001. Experimental study on a novel linear electromagnetic pumping unit. *IEEE Trans. Magn.*, **37**(1):219-222. [doi:10.1109/20.911825]

Qu, R.H., Lipo, T.A., 2002. Analysis and Modeling of Airgap & Zigzag Leakage Fluxes in a Surface-Mounted-PM Machine. Proc. 37th IAS Annual Meeting, p.2507-2513. [doi:10.1109/IAS.2002.1042798]

Rieder, U.H., Schroedl, M., 2005. A Simulation Method for Analyzing Saliencies with Respect to Enhanced Inform-capability for Sensorless Control of PM Motors in the Low Speed Range Including Standstill. European Conf. on Power Electronics and Applications. CD-ROM. [doi:10.1109/EPE.2005.219744]

Tang, R.Y., 1997. Modern Permanent Magnet Machines—Theory and Design. China Machine Press, Beijing, China, p.37-61 (in Chinese).

Yang, Y.B., Wang, X.H., Zhang, R., Ding, T.T., Tang, R.Y., 2006. The optimization of pole arc coefficient to reduce cogging torque in surface-mounted permanent magnet motors. *IEEE Trans. Magn.*, **42**(4):1135-1138. [doi:10.1109/TMAG.2006.871452]

Yu, F.P., Liu, X.Q., Gao, Z.Y., Chen, X.W., Jiao, T.J., Yang, N., 2005. Energy-saving effect test and analysis of permanent magnet motor in the pumping unit. *Oil Field Equip.*, **34**(1):83-85 (in Chinese).